RAIN RATE

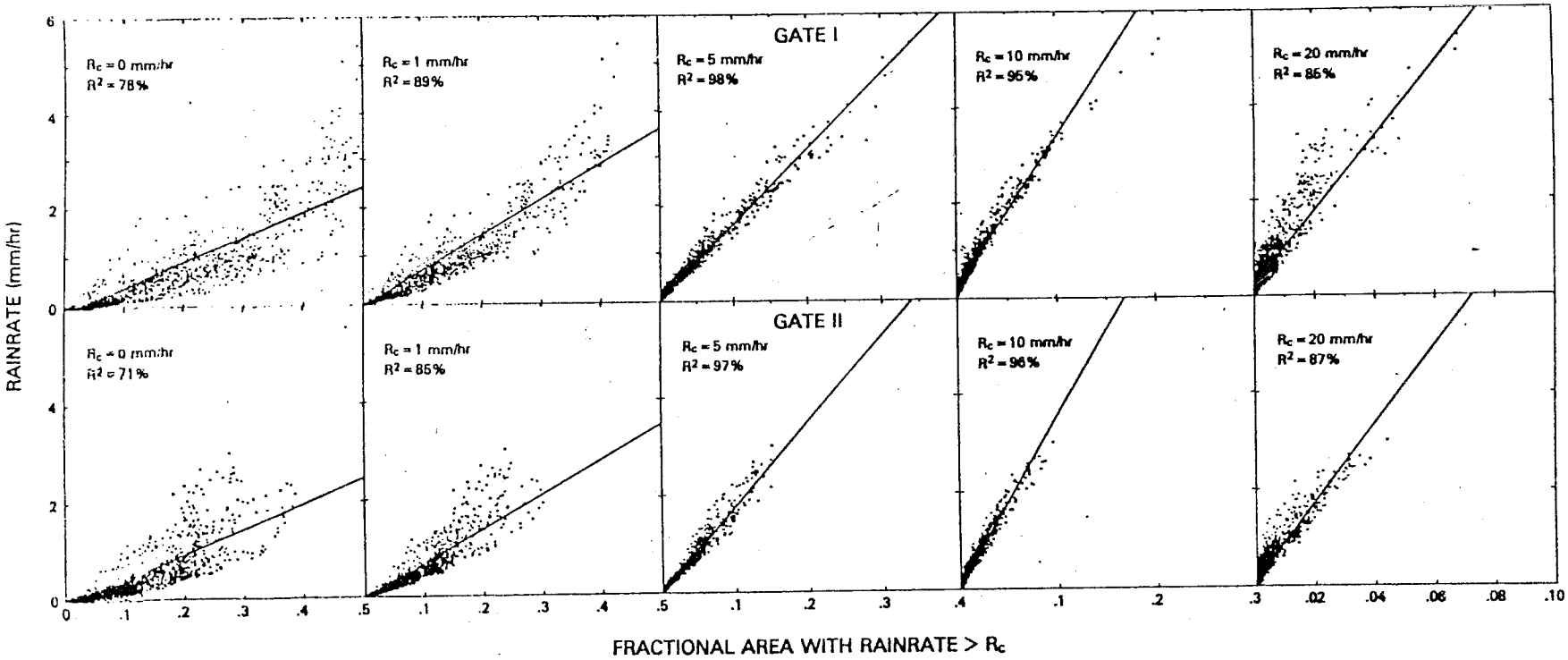

Figure 1. Scattergram and the corresponding linear regression of the area average rain rate on the fractional area.

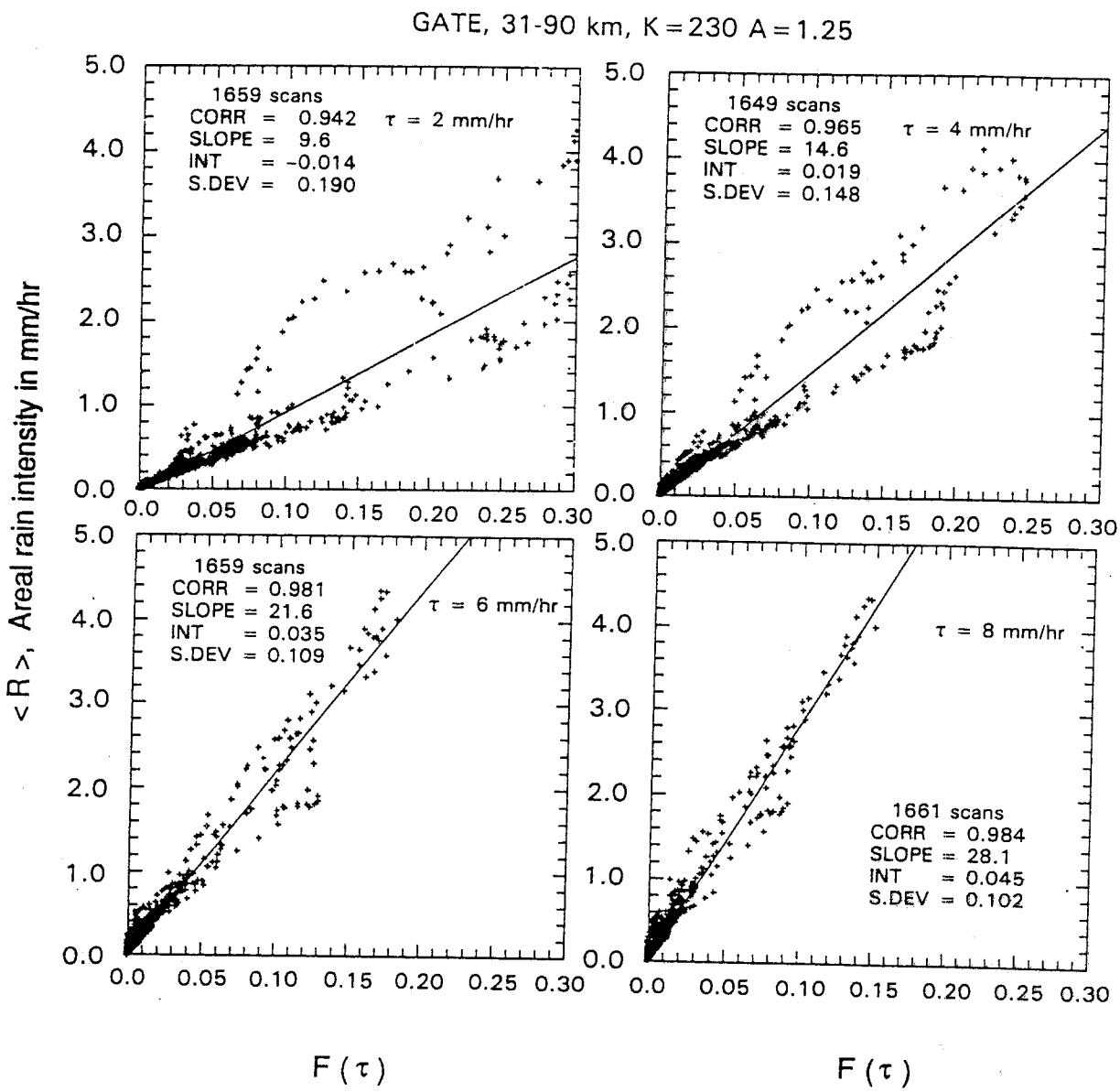

Fig. 1. The $\langle R \rangle$-$F(\tau)$ relation for GATE phase 3. Each point represents one radar scan. The ordinate is the averaged radar-derived rain rate ($\langle R \rangle$, in millimeters per hour) over the area between the 31- and 90-km range markers; the abscissa is the fraction of this area, $F(\tau)$, which is covered with rain intensities greater than a threshold τ equal to 2, 4, 6 and 8 mm/h for the four panels, as labeled.

$\tau = 5$ mm/h is $\phi = 0.62$ (see part 1) for the GATE pdf, then the climatological values of the average rain rate over the area covered by rain of at least 5 mm/h is $R_c = 9.9$ and 11.2 mm/h, respectively, for the two phases. R_c is the mean climatological rain rate within the area encompassed by the threshold rate τ. *Chiu* [1988*a*, *b*] did not attribute significance to the differences in $S(\tau)$ between the two periods, but this is a point which we must address later in determining the stability and accuracy of the method. The very large scatter which is evident at τ smaller than about 2 mm/h may be a result of one or more of the following factors: (1) stratiform rain probably lacks a consistent pdf of the rain intensities; (2) light rain is likely to produce larger variability in the Z-R relationship than heavier rain; (3) small intensities may be produced either by stratiform rain or by shallow convective cells.

Chiu also examined the spatial variability of the regressions by dividing the GATE area into four regions and using $\tau = 5$ mm/h for both phases. The slopes varied from 15.4 to 18.3 mm/h, suggesting a mean slope of 16.9 ± 1.5 to encompass variations in both space and time. Of course, more data are necessary to determine how stable these slopes and the corresponding pdf's are. Indeed, Chiu showed that the cumulative distributions of area covered by rain differed between the two phases of GATE; only 15% of the snapshots had fractional area coverage in excess of 0.2 in phase 2 compared to 25% in phase 1, thus accounting in part for the smaller slope in phase 1.

TABLE 1. Properties of the Cumulative Rain Volume Distributions for GATE (Phase 3), South Africa, and Texas

Locale	R, mm/h			Parameters of pdf and $\langle R\rangle$-$F(\tau)$ Relation for τ = 6 mm/h			
	10%	50%	90%	ϕ	R_c mm/h	$S(\tau)$ pdf	$\langle R\rangle/F(\tau)$, mm/h
GATE (phase 3)	1.3	9.3	39.	0.62	13.1	21.2	21.6
South Africa	1.6	12.	69.	0.66	16.7	25.3	27.4
Texas	2.0	18.	79.	0.75	18.5	24.7	25.8

relationships used for this study are those which are most commonly used for each of the three regions. The values are (1) South Africa, $Z = 200R^{1.4}$ [*Pasqualucci*, 1976], (2) Texas, $Z = 383R^{1.615}$ [*Smith et al.*, 1977], and (3) GATE, $Z = 230R^{1.25}$ [*Hudlow et al.*, 1979]. No Z-R relationships are established for Darwin. Since both Darwin and GATE are tropical maritime convective regimes, we also used the GATE Z-R relationship for Darwin.

Figure 2 shows the cumulative distributions for South Africa and Texas, and the inset table shows the various percentiles. Note that the rain rates at the 50% level increase from GATE, to South Africa, to Texas in agreement with the known progression of the vigor of the storms. Also, note that the fractional contribution to the total rain volume by rates in excess of 6 mm/h, the value of ϕ, also increases in a similar manner from 0.62 to 0.66 to 0.75. In Table 1 we list the various significant features of the cumulative distributions for the three regions along with the values of ϕ, the associ-

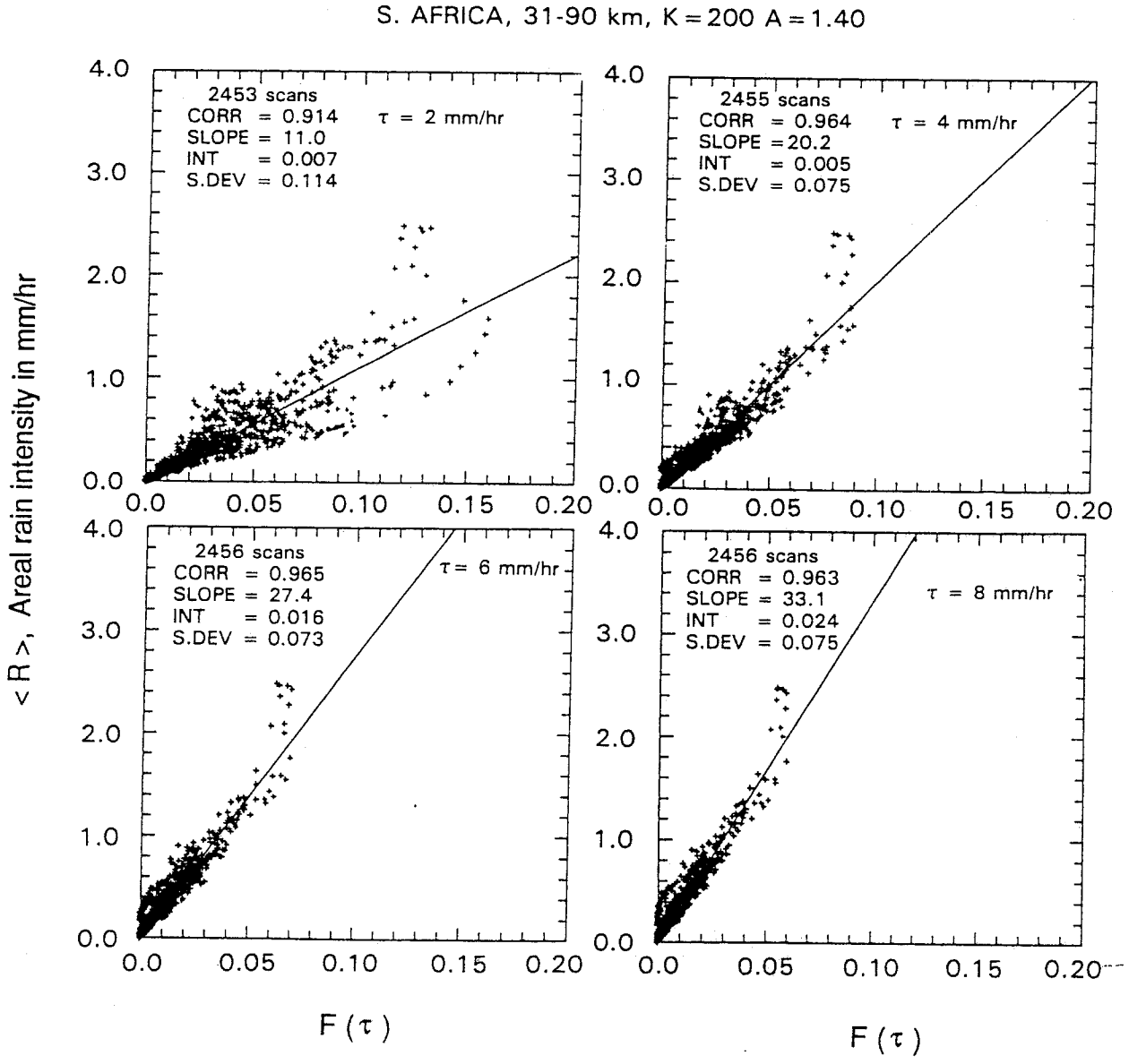

Fig. 3. The same as Figure 1, but for South Africa.

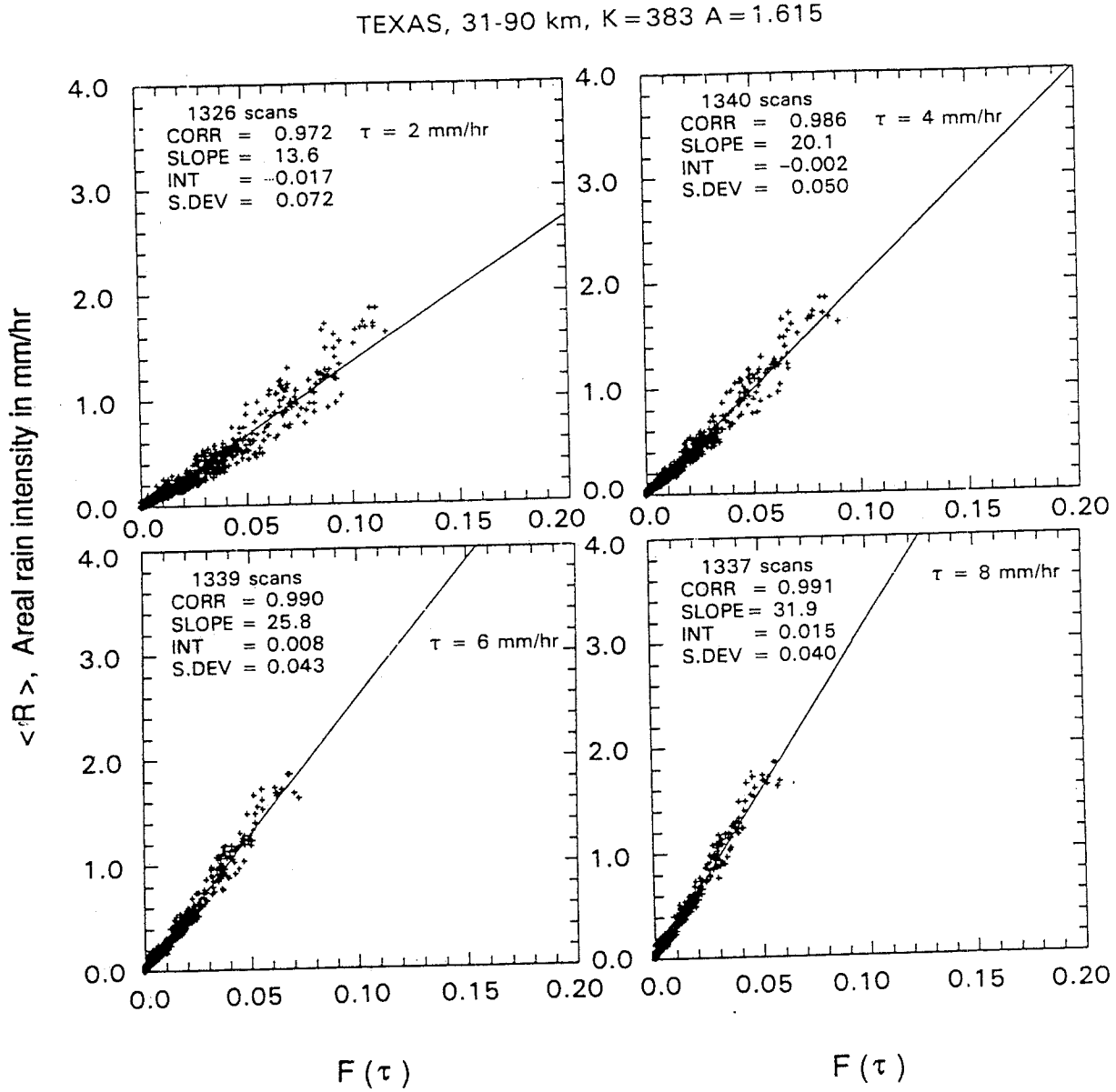

Fig. 4. The same as Figure 1, but for west Texas.

ated climatological rain rate R_c, and $S(\tau)$, all for a threshold $\tau = 6$ mm/h. Also shown are $S(\tau)$ calculated from the regression lines of $\langle R \rangle$ versus $F(\tau)$. R_c is calculated from $R_c = S(\tau)\phi$ (see part 1).

The comparison between the $S(\tau)$ calculated directly from the pdf's and the $S(\tau)$ as obtained from the $\langle R \rangle$-$F(\tau)$ relation, given in Table 1, shows good agreement between the two methods. This and the very high correlation of the $\langle R \rangle$-$F(\tau)$ relations indicate that the instantaneous distribution of rain rates in any snapshot satisfies the condition that $R_c/\phi \cong$ const for τ of 5–8 mm/h at all three locales. This is an important point which has been emphasized by Atlas et al. in part 1 because it allows one to use a relatively small sample to establish the climatological relation for the season.

Figures 3 and 4 show the $\langle R \rangle$-$F(\tau)$ scattergrams for South Africa and Texas, respectively. The correlations in these regions are even higher than in GATE. The tightest relations are those for Texas. The slopes $S(\tau)$ for 6 mm/h are given in Table 1 and agree well with the theoretical values of $S(\tau)$ based upon ϕ from the distribution in Figure 2. To complete the picture, we have examined some very recent data from Darwin, Australia. The $\langle R \rangle$-$F(\tau)$ scattergrams for all four areas for the single threshold of $\tau = 6$ mm/h are compared in Figure 5. We have only 48 snapshots from Darwin, but the small scatter about the regression line suggests that these data are indicative of the monsoon rain regime in Darwin. The high correlations in $\langle R \rangle$-$F(\tau)$ relations of the four different convective regimes suggest that this kind of analysis is valid universally for convective rain.

Figure 6, for $\tau = 1$ mm/h in Texas, conveys an important message since it shows a set of points along a much smaller slope than the rest of the data. All these points were found to occur on a single day on which stratiform rain fell from midlevels. This demonstrates that our approach is applicable to both the cellular and the stratiform regions of rain, but only if this rain has been initiated convectively. Because stratiform rain covers much larger areas with much smaller rain rates, any set of points which systematically underes-

Fig. 5. The ⟨R⟩-F(r) relations for South Africa, Texas, GATE phase 3, and Darwin, Australia. Each point represents one radar scan. The ordinate is the averaged radar-derived rain rate (⟨R⟩, in millimeters per hour) over the area between the 31- and 90-km range markers; the abscissa is the fraction of this area, F(r), which is covered with rain intensities greater than a threshold r equal to 6 mm/h.

timates ⟨R⟩ significantly relative to the value given by the climatological relation for convective rain can automatically be attributed to stratiform conditions.

In Figure 7 we plot curves of the slope S(r) versus threshold r for all four regimes and for all r from 1 to 10 mm/h. Interestingly, S(r) increases essentially linearly with r for all four regions. Of course, the larger S(r), the more rain is produced in the whole domain per unit storm area with R > r. Although the cumulative distributions of Figure 2 showed greater median rain rates in Texas than in South Africa, the reverse is true for S(r), the rate per unit area, at least for r = 4 mm/h. On the other hand, above r = 4 mm/h, S(r) increases progressively from Darwin to GATE to Texas, to South Africa. This is opposite to the progression of the cloud base temperatures, which are as follows: Darwin, 24°C; Texas, 16°C; and South Africa, 8°C. Additionally, Figure 5 shows that the largest values of the fraction of area covered by rain in a given locale, as indicated by F(r), also increases with increasing cloud base temperature. These observations seem to be consistent with the fact that as we move to increasingly more tropical and maritime areas, warm rain processes become more efficient. Thus, there is an increased frequency of small but light showers, so that the total rain is distributed over a larger area encompassed by the rainy cells or echoes. These observations may also suggest that the portion of the stratiform rain in convective situations generally increases with warmer cloud base temperature.

It is encouraging that both the cumulative distributions and the slopes of the ⟨R⟩-F(r) regression lines behave in such a physically and climatologically plausible manner. This

Table 1. Minimum χ^2-estimates from different designs. Source: Kedem et al.(1990b).

GATE	*Design*	$\hat{\mu}$	$\hat{\sigma}$
	(2,4,4)	1.137	1.043
	(2,8,8)	1.157	1.031
	(4,4,4)	1.129	1.048
	(4,8,8)	1.140	1.039
	(5,20,20)	1.185	1.033
	(6,6,6)	1.152	1.028
	(6,8,8)	1.169	1.042
I	(8,4,4)	1.126	1.045
	(8,6,6)	1.182	1.030
	(10,8,8)	1.162	1.029
	(10,10,10)	1.085	1.084
	(20,10,10)	1.095	1.035
	(24,1,1)	1.159	1.028
	(48,1,1)	1.255	1.009
	(4,4,4)	1.065	1.100
	(3,10,10)	1.032	1.100
	(5,3,3)	1.099	1.077
	(5,5,5)	1.056	1.091
	(5,10,10)	1.031	1.089
	(8,8,8)	1.046	1.053
II	(10,5,5)	1.043	1.098
	(10,10,10)	0.960	1.161
	(20,3,3)	1.050	1.098
	(20,5,5)	0.998	1.121
	(20,10,10)	0.918	1.180
	(30,5,5)	0.976	1.123
	(30,10,10)	0.982	1.214
	(48,1,1)	1.041	1.028

Or: minimize

$$S_\theta(u(\tau)) = w_\theta(\tau) =$$

$$S_\theta(u) \equiv \frac{\sigma^2}{[1-\Phi(u)]^2}\{[1-\Phi(u)-\frac{1}{\sigma}\phi(u)]^2+\frac{1}{2}[\sigma(1-\Phi(u))-\frac{u}{\sigma}\phi(u)]^2\}$$

$$u = (\log\tau - \mu)/\sigma$$

For GATE-like rain:

$$\theta = (1,1)$$

The minimum occurs at

$$\tau^*_{opt} = 5.1309$$

This is the optimal threshold by Procedure 2.

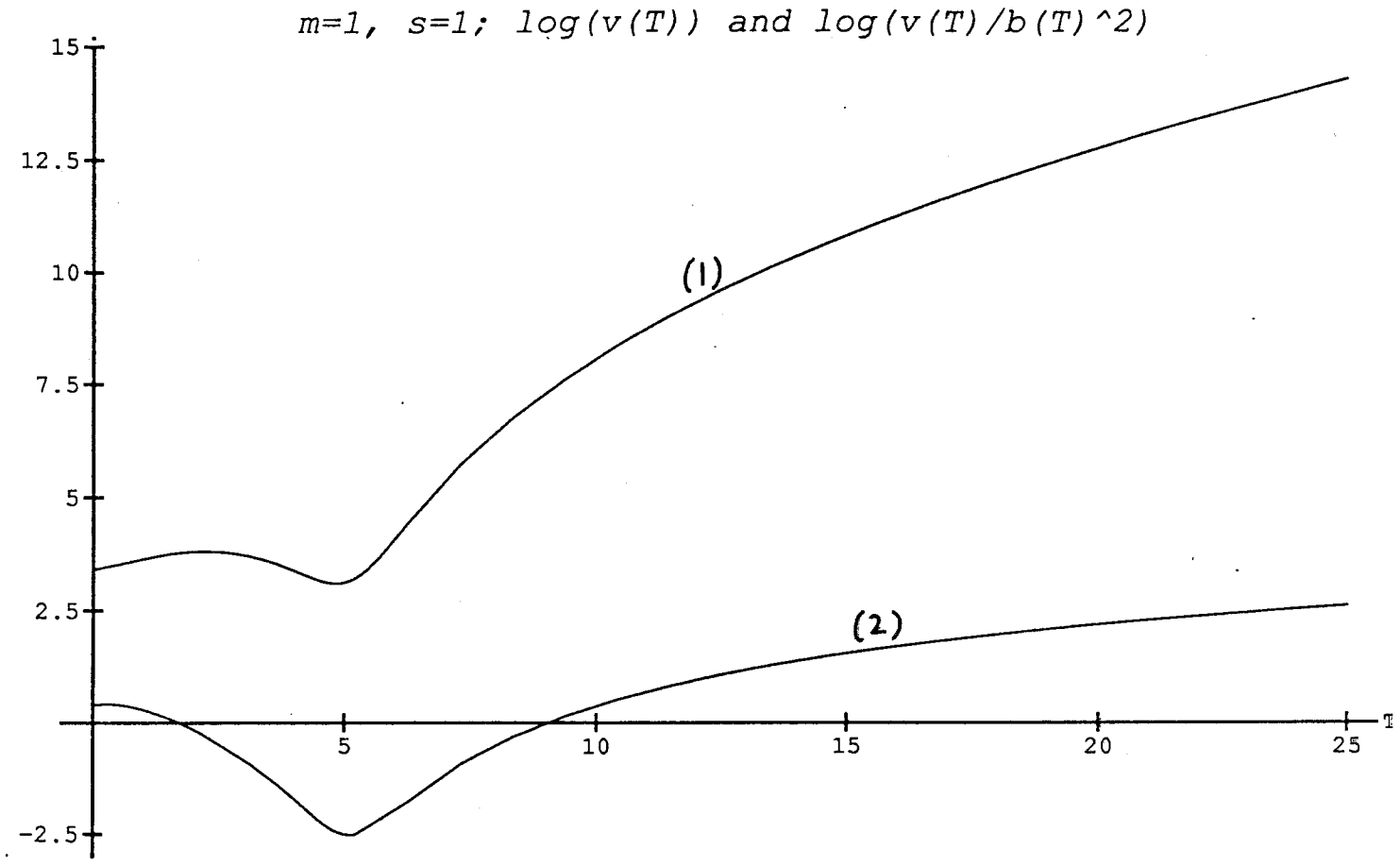

Figure 4. Comparison of Procedure 1 with Procedure 2 in the lognormal case $\Lambda(1,1)$. $\tau_{opt} < 5 < \tau^*_{opt}$.